

Cosmic bulk flows on $50 h^{-1}\text{Mpc}$ scales: A Bayesian hyper-parameter method and multishell likelihood analysis

Yin-Zhe Ma^{1,2,†} & Douglas Scott^{1,*}

¹*Department of Physics and Astronomy, University of British Columbia, Vancouver, V6T 1Z1, BC Canada.*

²*Canadian Institute for Theoretical Astrophysics, Toronto, M5S 3H8, Ontario, Canada.*

*emails: †mayinzhe@phas.ubc.ca; *dscott@phas.ubc.ca*

7 November 2018

ABSTRACT

It has been argued recently that the galaxy peculiar velocity field provides evidence of excessive power on scales of $50 h^{-1}\text{Mpc}$, which seems to be inconsistent with the standard ΛCDM cosmological model. We discuss several assumptions and conventions used in studies of the large-scale bulk flow to check whether this claim is robust under a variety of conditions. Rather than using a composite catalogue we select samples from the SN, ENEAR, SFI++ and A1SN catalogues, and correct for Malmquist bias in each according to the *IRAS* PSCz density field. We also use slightly different assumptions about the small-scale velocity dispersion and the parameterisation of the matter power spectrum when calculating the variance of the bulk flow. By combining the likelihood of individual catalogues using a Bayesian hyper-parameter method, we find that the joint likelihood of the amplitude parameter gives $\sigma_8 = 0.65_{-0.35}^{+0.47}$ (68 per cent confidence region), which is entirely consistent with the ΛCDM model. In addition, the bulk flow magnitude, $v \sim 310 \text{ km s}^{-1}$, and direction, $(l, b) \sim (280^\circ \pm 8^\circ, 5.1^\circ \pm 6^\circ)$, found by each of the catalogues are all consistent with each other, and with the bulk flow results from most previous studies. Furthermore, the bulk flow velocities in different shells of the surveys constrain (σ_8, Ω_m) to be $(1.01_{-0.20}^{+0.26}, 0.31_{-0.14}^{+0.28})$, for SFI++ and $(1.04_{-0.24}^{+0.32}, 0.28_{-0.14}^{+0.30})$ for ENEAR, which are consistent with *WMAP* 7-year best-fit values. We finally discuss the differences between our conclusions and those of the studies claiming the largest bulk flows.

Key words: methods: statistical–galaxies: kinematics and dynamics –distance scale–large-scale structure of Universe

1 INTRODUCTION

The cosmic bulk flow is the streaming motion of the galaxies surrounding our Milky Way system, due to the gravitational pull of cosmic structure on large scales. In the gravitational instability paradigm, for a galaxy at position \mathbf{r} , the peculiar velocity of an individual galaxy at time t is given by (Peebles 1993)

$$\mathbf{v}(\mathbf{r}, t) = \frac{\Omega_m^{0.55} H_0}{4\pi} \int d^3 \mathbf{r}' \delta_m(\mathbf{r}', t) \frac{\mathbf{r} - \mathbf{r}'}{|\mathbf{r} - \mathbf{r}'|^3}, \quad (1)$$

where $\delta_m(\mathbf{r}) = (\rho(\mathbf{r}) - \bar{\rho})/\bar{\rho}$ is the density contrast at position \mathbf{r} , Ω_m is the fractional matter density, and H_0 is the Hubble constant. The bulk flow is normally considered as an average over a sufficiently large volume, with some window function $w(r, R)$, so that the above linear perturbation theory is applicable. This average is defined as (Juszkiewicz

et al. 1990; Nusser & Davis 2011)

$$\mathbf{V}_{\text{bulk}}(\mathbf{r}, t) = \frac{\int d^3 \mathbf{r}' \mathbf{v}(\mathbf{r}', t) w(|\mathbf{r}' - \mathbf{r}|, R)}{\int d^3 \mathbf{r}' w(|\mathbf{r}' - \mathbf{r}|, R)}, \quad (2)$$

where $\mathbf{v}(\mathbf{r}, t)$ is the 3-D peculiar velocity field at time t , defined in Eq. (1). A complete investigation of bulk flows of nearby galaxies should measure the individual velocities of galaxies all over the observed volume. However, realistic observational techniques, such as the Tully-Fisher relation, only allow us to probe the radial component of the peculiar velocities of galaxies. In addition, most of the current observations can only cover a patch of sky with limited depth, leading to large uncertainties when interpreting the results.

Of course, none of these considerations are new. There is already a large literature on the study of the peculiar velocity field, with particularly intense activity in the early 1990s (see overviews in Burstein 1990; Courteau et al. 1993; Latham & da Costa 1991; Bouchet & Lachièze-Rey M. 1993; Strauss & Willick 1995; Courteau & Willick 2000). Investi-

gating the relationship between velocities and densities has great potential for constraining cosmological parameters, and testing theories of gravity on large scales. However, it has long been realised that the construction of appropriate catalogues is difficult, and that systematic effects can easily overwhelm statistical noise.

In attempting to overcome these observational limitations, there have been significant recent efforts in the community to reconstruct bulk flow moments from the limited data available, and to test their consistency with the Λ CDM cosmology. One of the important issues lies in determining the proper weighting for individual galaxy velocities in a catalogue in order to obtain streaming motions. Some of the published studies, such as Sarkar et al. (2007) and Abate & Erdogdu (2009), focus on a weighting scheme that produces the maximum likelihood estimate of the bulk flow (see also Watkins et al. 2009), which can minimise the measurement noise. However, this weighting depends on the particular survey geometry and statistical properties, which leads to a large uncertainty when interpreting the constraints from combined data sets.

Watkins et al. (2009) proposed another method of estimating the bulk flow of galaxy peculiar velocities. They focused on the problem of how realistic surveys can be used to reconstruct the bulk flow at a given depth. They developed a minimum variance weighting method (Watkins et al. 2009; Feldman et al. 2010), which minimises the variance between the real data catalogue and the ideal survey, and they applied it to combined catalogues of peculiar velocity surveys. Surprisingly, they found a very large bulk flow on $50 h^{-1}$ Mpc scales ($v = 407 \pm 81 \text{ km s}^{-1}$) towards $l = 287^\circ \pm 9^\circ$, $b = 8^\circ \pm 6^\circ$, which prefers a large amplitude of fluctuations (σ_8), inconsistent with the *WMAP* 5-year results (Komatsu et al. 2009). Subsequent work has discussed a possible explanation for this large bulk flow related to pre-inflationary isocurvature perturbations (Ma et al. 2011).

Contradicting the claim in Watkins et al. (2009), Nusser & Davis (2011) developed a method termed the ASCE (All Space Constrained Estimate) which reconstructs the bulk flow from an all-space 3-D velocity field to match the inverse Tully-Fisher relation. By applying this method, as well as the Maximum likelihood method (Abate & Erdogdu 2009), to the Spiral Field *I*-band Survey (SFI++ survey, Springob et al. 2007) catalogue, Nusser & Davis (2011) found the bulk flow on a sphere of $40 h^{-1}$ Mpc radius to be $v = 333 \pm 38 \text{ km s}^{-1}$, towards $(l, b) = (276^\circ \pm 3^\circ, 14^\circ \pm 3^\circ)$, which is close to the results from the maximum likelihood method. The estimated cosmological parameters, i.e. $(\Omega_m, \sigma_8) = (0.236, 0.88)$, are consistent with the Λ CDM model. However, since Nusser & Davis (2011) only used the SFI++ data set, it is still not clear whether it is the other data sets used in Watkins et al. (2009) which led to the significantly different results.

Any analysis which claims to strongly rule out the simple inflationary Λ CDM model deserves careful scrutiny, since a confirmed discordance would have profound consequences for our understanding of the large-scale Universe. We can identify four potential problems in Watkins et al. (2009) which may potentially skew the likelihood and bias the results. Firstly, the inhomogeneous Malmquist bias is not corrected for in most catalogues, for example: ENEAR (da Costa et al. 2000; Bernardi et al. 2002; Wenger et al. 2003);

SN (Tonry et al. 2003); SC (Giovanelli et al. 1998); EFAR (Colless et al. 2001); and Willick (Willick 1999). This deficiency can significantly bias the distance estimates. Secondly, the distance errors from the Tully-Fisher and Fundamental Plane methods can be comparable to the measured velocities as the surveys go deeper, and moreover a simple model of Gaussian errors is almost certainly inappropriate as systematics come to dominate the distance estimation. Therefore the velocity data beyond $100 h^{-1}$ Mpc become both very noisy and unreliable in assessing the bulk flow. Thirdly, directly combining various catalogues with different calibration methods can also induce systematic errors and a spurious flow. Finally, the assumption of a unique small scale velocity dispersion $\sigma_* = 150 \text{ km s}^{-1}$ may be too small for some of the surveys (e.g. SFI++ prefers 400 km s^{-1} , Ma et al. 2011), perhaps skewing the constraints on the cosmological parameters σ_8 and Ω_m . The purpose of this paper is to investigate carefully the analysis presented in Watkins et al. (2009), and to combine each catalogue with a Bayesian hyper-parameter method to test for consistency with the usual Λ CDM perturbation theory. As we have seen from Nusser & Davis (2011), different statistical methods should not dramatically alter the results, so we will focus on the ‘minimal variance’ scheme (Watkins et al. 2009; Feldman et al. 2010).

A further motivation for this paper is as an extension to the velocity-gravity comparison work we have already carried out in Ma et al. (2012b). In that paper we compare the observational peculiar velocity data with the reconstructed velocity field from the *IRAS* PSCz catalogue, and fit the linear growth rate parameter, β . In this new paper, we do not discuss the small-scale modes, but will reconstruct the bulk motion of galaxies on distances $\sim 50 h^{-1}$ Mpc. We will perform a direct comparison between observational data and Λ CDM model predictions for the bulk flow velocity, and constrain the cosmological parameters σ_8 and Ω_m . In addition, we will extend the minimal variance scheme suggested in Watkins et al. (2009) and Feldman et al. (2010) to a multishell likelihood method. Furthermore, we will directly investigate the reason for the apparently large flows found in Watkins et al. (2009) and Feldman et al. (2010).

This paper is organised as follows. We first list the data sets used in Section 2.1, and then discuss the data selection criterion in Section 2.2. For the selected data, we correct the inhomogeneous Malmquist bias for the distance estimate (Section 2.3). In Section 3, we first illustrate how to quantify the variance of the bulk flow at any particular depth (Section 3.1), then we review the minimum variance weighting scheme proposed in Watkins et al. (2009) to measure the bulk flow at a given depth (Section 3.2), and furthermore we present the likelihood function for each individual catalogue (Section 3.3) and the hyper-parameter approach used to combine different data sets (Section 3.4). Then in Section 4 we compare our findings with those in Watkins et al. (2009). We first confirm that we can accurately reproduce the results in Watkins et al. (2009) by adopting the same conventions; then in Section 4.1 we show our constraints on bulk flow moments by performing the full likelihood analysis for each individual catalogue rather than the combined catalogue. In Section 4.2, we apply the Bayesian hyper-parameter method to combine the likelihoods of different catalogues, in order to avoid the systematics that may affect the constraints.

This allows us to assess the consistency of each individual catalogue, and to work out the cosmological parameters in the combined likelihood. In Section 4.3, we extend our likelihood analysis to consider bulk flows in multiple shells in a survey, and their covariance matrix, and we compare our findings with *WMAP* 7-year best-fit values and the results from Nusser & Davis (2011). Our discussion and conclusion are summarised in Section 5.

Note that although H_0 ($= 100h \text{ km s}^{-1} \text{ Mpc}^{-1}$) is now determined with reasonable accuracy, throughout this paper we continue to adopt the convention of giving distances in units of $h^{-1} \text{ Mpc}$ for ease of comparison with previous results.

2 DATA

2.1 Catalogues

We will use four different samples coming from recent peculiar velocity surveys to reconstruct the bulk flow. These samples are listed from the nearest to the most distant (see also Watkins et al. 2009; Feldman et al. 2010; Turnbull et al. 2012). Our four samples consist of the ENEAR catalogue (da Costa et al. 2000; Bernardi et al. 2002; Wenger et al. 2003; Hudson 1994), the SN catalogue (Tonry et al. 2003), the SFI++ catalogue (Springob et al. 2007) and the A1SN catalogue (Turnbull et al. 2012; Jha et al. 2007; Hicken et al. 2009; Folatelli et al. 2010). For detailed discussion and analyses of these four samples, including their characteristic depths, typical distance errors and data compilation, we refer readers to Section 3 of Ma et al. 2012b.

We should mention that in Watkins et al. (2009) and Feldman et al. (2010) five other catalogues, namely SBF (Tonry et al. 2001), SC (Giovanelli et al. 1998; Dale et al. 1999), SMAC (Hudson 1999; Hudson et al. 2004), EFAR (Colless et al. 2001) and Willick (Willick 1999), were used to reconstruct the bulk flow of galaxies. In contrast to the previously described four catalogues, these samples are either very distant and therefore have large errors, or very sparse in which case the survey geometry is complicated. Watkins et al. (2009) combined these five low-quality catalogues with the previous four higher quality catalogues to form a larger ‘COMPOSITE’ catalogue, and found an excess power of flow on scales of $50 h^{-1} \text{ Mpc}$. However, there is potential danger in combining various catalogues with different calibration schemes. One concern is that the very distant samples with large systematics may be inducing a spurious large-scale flow.

In order to investigate this we tried to reproduce the ‘excess flow’ effect by using the suspicious COMPOSITE catalogue (see Section 3). However, in the subsequent more careful analysis, we will only use the ENEAR, SN, A1SN and SFI++ catalogues, with the following data selection criterion and Malmquist bias correction.

2.2 Data selection

We listed four different peculiar velocity catalogues in Section 2.1. In these catalogues, the samples beyond the $80 h^{-1} \text{ Mpc}$ scale are also quite sparse and suffer from large

	$d \leq 80$	$80 \leq d \leq 200$
ENEAR	669	28
SN	78	25
SFI++	2404	1052
A1SN	153	92

Table 1. Peculiar velocity samples. The two columns give the number of galaxies within the range $d \leq 80 h^{-1} \text{ Mpc}$ (used in this paper) and $80 < d < 200 h^{-1} \text{ Mpc}$ (considered as outliers).

errors due to uncertainties in the distance indicators; therefore we trim the data sets at $80 h^{-1} \text{ Mpc}$ in order to reconstruct the bulk flow moments accurately on the $50 h^{-1} \text{ Mpc}$ scale.

In addition, since some of the samples in the SFI++ catalogue with $d \lesssim 30 h^{-1} \text{ Mpc}$ are affected by localised non-linear structures, giving very large velocities (Ma et al. 2012b), we excluded these high velocity samples ($|v| > 3000 \text{ km s}^{-1}$) from the SFI++ catalogue. The classification of the data in each catalogue is listed in Table 1.

2.3 Malmquist bias correction

In the above description of velocity catalogues, two different distance indicators, the Tully-Fisher relation and the Fundamental Plane method, have been used for determining the SFI++ and ENEAR distances. In addition, supernova luminosities are used in calibrating the distance of the SN and A1SN catalogues.

The large scatter of distance indicators suggests that objects with inferred distance d , may come from a wide range of possible true distances. The effect usually referred to as Malmquist bias (Malmquist 1920; Hendry et al. 1993) is related to the probability distribution of true distance r , given the measured distance d with its measurement error. The desired function is (Lynden-Bell et al. 1988a; Strauss & Willick 1995)

$$P(r|d) = \frac{r^2 n(r) \exp\left(-\frac{[\ln(r/d)]^2}{2\Delta^2}\right)}{\int_0^\infty dr r^2 n(r) \exp\left(-\frac{[\ln(r/d)]^2}{2\Delta^2}\right)}, \quad (3)$$

where $n(r)$ is the radial density distribution, and $\Delta = (\ln(10)/5)\sigma \simeq 0.46\sigma$ is the fractional distance uncertainty of distance indicators. Note that for the Tully-Fisher and Fundamental Plane methods, the typical errors are around 20 per cent, and for Type Ia supernovae, the typical error is around 6–8 per cent.

The simplest case is *homogeneous Malmquist bias* (Strauss & Willick 1995; Hudson 1994), in which, the number density is constant, so that Eq. (3) becomes independent of density, with

$$P(r|d) = \frac{1}{\sqrt{2\pi}(d\Delta)} \exp\left(-\frac{9}{2}\Delta^2\right) \left[x^2 \exp\left(-\frac{[\ln x]^2}{2\Delta^2}\right) \right], \quad (4)$$

where $x = r/d$ is the ratio between the true distance and the measured distance. One can verify that the expectation of r , $E(r|d) = \int r P(r|d) dr = d e^{7\Delta^2/2}$. This means that even for a constant density distribution of galaxies, the distance indicator is still generally biased. This is due to the fact that, near the measured distance d , there are more galaxies in shells of larger distance than smaller distance, so it is more

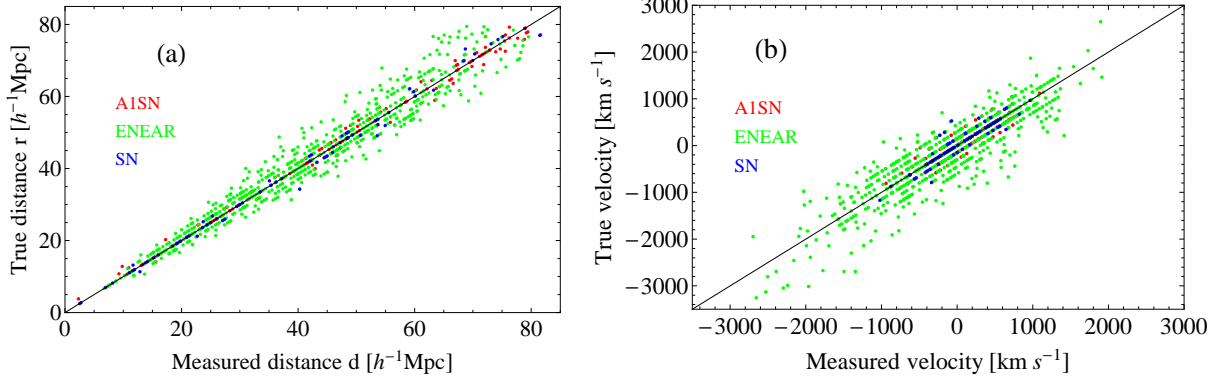


Figure 1. Inhomogeneous Malmquist bias correction. The $n(r)$ function of Eq. (3) is interpolated by using *IRAS* PSCz density samples.

probable that the true distance is greater than the measured distance i.e. $E(r|d) > d$.

However, in the more general case, the gradient of the number density is not negligible, and this either reinforces or works against the volume effect – *inhomogeneous Malmquist bias*. If the gradient of the number density is positive, there will be even more galaxies at the larger distances than in the constant density case, i.e. the inhomogeneity reinforces the homogeneous Malmquist bias; on the other hand, if the gradient is negative, then the effective is opposite, and the inhomogeneous Malmquist bias partially cancels the homogeneous Malmquist bias effect.

To quantify the inhomogeneous Malmquist bias correctly, we use the real-space reconstructed positions of the PSCz galaxies as mass tracers to interpolate the mass density field on a cubic grid of Length $192 h^{-1} \text{Mpc}$ and mesh size $1.5 h^{-1} \text{Mpc}$, smoothed with a Gaussian filter of $5 h^{-1} \text{Mpc}$. The field on the lattice is then interpolated along the line of sight to each object in the catalogue. The value of $n(r)$ along the line of sight is specified at the position of 21 equally-spaced points, with a binning of $1.5 h^{-1} \text{Mpc}$. Finally, Eq. (3) is used to predict r from d using a Monte Carlo rejection procedure.

We re-examine the catalogues described in Section 2.1, and correct for Malmquist bias according to Eq. (3) for the ENEAR, SN and A1SN samples¹. We plot the measured distance (before Malmquist bias correction) and corresponding true distance (after Malmquist bias correction) in the left panel of Fig. 1. One can see that removing the bias tends to place galaxies at larger distances, although the shift is not very significant. The right panel of Fig. 1 shows the comparison between the uncorrected and corrected line-of-sight peculiar velocities.

3 MEASURING THE BULK FLOW

For linear perturbation theory within the ΛCDM paradigm, the velocity field at any spatial point $\mathbf{v}(\mathbf{r}, t)$ is directly related to the underlying density field through Eq. (1). What we are interested in is the bulk flow moment of the velocity field in a spherical region. Therefore in this section, we

first calculate the mean-squared variance of the bulk flow (in Eq. (2)) which can be used to quantify the amplitude of the flow at different depths. Then we will review the ‘minimum variance’ method for weighting the data sets on different scales. Finally we will present the likelihood function that can be used to constrain cosmology with the measured bulk flow.

3.1 Mean-squared velocity in a top-hat region

Real surveys can only observe galaxies out to a particular depth R , which means that the ‘window function’ has a sharp cut-off:

$$w(|\mathbf{r}' - \mathbf{r}|, R) = \begin{cases} 0, & \text{if } |\mathbf{r}' - \mathbf{r}| > R; \\ 1, & \text{if } |\mathbf{r}' - \mathbf{r}| \leq R. \end{cases} \quad (5)$$

Therefore, by measuring only a galaxy sample within this sphere of radius R , one can calculate the ‘streaming motion’ through Eq. (2) by averaging the velocity within the sphere. The mean-squared velocity of the spherical region within radius R is therefore (see also Ma et al. 2012a)

$$\begin{aligned} \langle |\mathbf{v}_{\text{bulk}}(t)|_R^2 \rangle &= \langle \mathbf{v}_{\text{bulk}}(\vec{x}, t)_R \cdot \mathbf{v}_{\text{bulk}}(\vec{x}, t)_R \rangle_{\vec{x} \text{ all space}} \\ &= \left(\frac{3}{4\pi R^3} \right)^2 \frac{(H_0 \Omega_m^{0.55} a(t))^2}{(2\pi)^3} \int d^3 \vec{k} \tilde{w}^2(k, R) \frac{P(k)}{k^2} \\ &= \frac{(3H_0 \Omega_m^{0.55} a(t))^2}{2\pi^2} \int P(k) \left(\frac{j_1(kR)}{kR} \right)^2 dk. \end{aligned} \quad (6)$$

At the present epoch $H = H_0$ and $a = 1$, so today

$$\langle |\mathbf{v}_{\text{bulk}}|_R^2 \rangle = \frac{(3H_0 \Omega_m^{0.55})^2}{2\pi^2} \int P(k) \left(\frac{j_1(kR)}{kR} \right)^2 dk. \quad (7)$$

We expect Eq. (7) to be useful for quantifying the non-zero velocity fluctuations of our local surroundings. For the *WMAP* 7-year cosmological parameters (Komatsu et al. 2011), the typical bulk flow magnitude on a scale of $50 h^{-1} \text{Mpc}$ from Eq. (7) is 310 km s^{-1} . We will compare this theoretical value with the measured velocity catalogues.

3.2 Minimum variance scheme

Bulk flow estimates are essentially weighted averages of the individual velocities in a galaxy survey (Watkins et al. 2009). Previous work, such as Abate & Erdogdu (2009) and Sarkar

¹ The SFI++ catalogue (Springob et al. 2007) was already corrected for Malmquist bias.

et al. (2007), focused on the estimate that minimises the uncertainties due to measurement noise, i.e. the maximum likelihood estimation scheme, but did not make any correction for the survey geometry. Thus the maximum likelihood bulk flow is obviously dependent on a given survey's particular geometry and statistical properties. On the other hand, Watkins et al. (2009) and Feldman et al. (2010) instead addressed the question of how peculiar velocity data can be used to statistically estimate a more specialised quantity, the bulk flow of an ideal, densely-sampled survey with a given depth. They developed a 'minimal variance' weighting scheme which produces an estimate of the bulk flow at any particular depth. They found an excess in the power of the bulk flow on scales of $50 h^{-1} \text{Mpc}$, which seems to exceed the ΛCDM predictions at the 3σ level. In the following, we will first review the minimum variance weighting scheme developed in Watkins et al. (2009) and Feldman et al. (2010) and then present the likelihood function for cosmological parameters.

A realistic survey consists of N objects on the sky having position \mathbf{r}_i and measured line-of-sight velocity S_i , with measurement error σ_i . The measured line-of-sight velocity is assumed to have the form $S_i = v_i + \delta_i$, where v_i is the galaxy line-of-sight velocity in the matter rest frame, and δ_i is a superimposed Gaussian random motion with variance $\sigma_i^2 + \sigma_*^2$, where σ_* accounts for the 1-D small-scale velocity dispersion.

Given an idealised survey with bulk flow velocity U_p ($p = 1, 2, 3$) at a particular depth R , we need to determine the weight $w_{p,i}$ which makes the 'linear compression'

$$u_p = \sum_{i=1}^N w_{p,i} S_i, \quad (8)$$

give the closest approximation of U_p (Feldman et al. 2010). At the same time, the line-of-sight velocity at position \mathbf{r}_i should take the form $v_i = \sum_p U_p (\mathbf{x}_p \cdot \mathbf{r}_i)$. In order for the estimator u_p to give the correct amplitude of the velocity U_p , i.e. $\langle u_p \rangle = U_p$, the weight function $w_{p,i}$ has to satisfy the following constraint:

$$\sum_i w_{p,i} (\mathbf{x}_q \cdot \mathbf{r}_i) = \delta_{pq}. \quad (9)$$

We can apply the Lagrange multiplier approach to minimise the average variance $\langle (u_p - U_p)^2 \rangle$, i.e. minimise the following quantity (Feldman et al. 2010)

$$\langle (u_p - U_p)^2 \rangle + \sum_q \left(\sum_i w_{p,i} (\mathbf{x}_q \cdot \mathbf{r}_i) - \delta_{pq} \right). \quad (10)$$

By plugging in Eq. (8), one can expand the first term and obtain

$$\begin{aligned} \langle U_p^2 \rangle - 2 \sum_i w_{p,i} \langle S_i U_p \rangle + \sum_{i,j} w_{p,i} w_{p,j} \langle S_i S_j \rangle \\ + \sum_q \lambda_{pq} \left(\sum_i w_{p,i} (\mathbf{x}_q \cdot \mathbf{r}_i) - \delta_{pq} \right). \end{aligned} \quad (11)$$

In order to find the weight function $w_{p,i}$ that can minimise the variance, we take the derivative of the above equation

and equate it to zero:

$$-2 \langle S_i U_p \rangle + 2 \sum_j w_{p,j} \langle S_i S_j \rangle + \sum_q \lambda_{pq} (\mathbf{x}_q \cdot \mathbf{r}_i) = 0. \quad (12)$$

From Eq. (12), one can solve for the weight function $w_{p,i}$ as

$$w_{p,i} = \sum_j (G^{-1})_{ij} \left[\langle S_j U_p \rangle - \frac{1}{2} \lambda_{pq} (\mathbf{x}_q \cdot \mathbf{r}_j) \right], \quad (13)$$

where $G_{ij} = \langle S_i S_j \rangle$ is the covariance matrix for the measured velocity. Since $S_i = v_i + \delta_i$ as described above, one can write the covariance matrix G as

$$\begin{aligned} G_{ij} &= \langle v_i v_j \rangle + \delta_{ij} (\sigma_*^2 + \sigma_i^2) \\ &= \langle (\hat{\mathbf{r}}_i \cdot \mathbf{v}(\mathbf{r}_i)) (\hat{\mathbf{r}}_j \cdot \mathbf{v}(\mathbf{r}_j)) \rangle + \delta_{ij} (\sigma_*^2 + \sigma_i^2), \end{aligned} \quad (14)$$

since v_i and δ_i are not correlated. The first term is the real space velocity correlation function, which is related to the matter power spectrum in Fourier space,

$$\langle (\hat{\mathbf{r}}_i \cdot \mathbf{v}(\mathbf{r}_i)) (\hat{\mathbf{r}}_j \cdot \mathbf{v}(\mathbf{r}_j)) \rangle = \frac{\Omega_m^{1.1} H_0^2}{2\pi^2} \int dk P(k) F_{ij}(k), \quad (15)$$

where the window function,

$$F_{ij}(k) = \int \frac{d^2 \hat{\mathbf{k}}}{4\pi} (\hat{\mathbf{r}}_i \cdot \hat{\mathbf{k}}) (\hat{\mathbf{r}}_j \cdot \hat{\mathbf{k}}) \times \exp(ik \hat{\mathbf{k}} \cdot (\mathbf{r}_i - \mathbf{r}_j)), \quad (16)$$

can be calculated analytically (Ma et al. 2011).

The correlation term $\langle S_j U_p \rangle$ is the average product of measured velocity S_j with the ideal bulk flow moment U_p . The ideal bulk flow moment U_p is the average of the random velocities in an isotropic survey region. We assume that the survey is a spherical region with radius R , therefore we generate $N' = 10^4$ random velocities in the top-hat region R and calculate $\langle S_j U_p \rangle$ as

$$\langle S_j U_p \rangle = \frac{1}{N'} \sum_{n'=1}^{N'} (\mathbf{x}_p \cdot \mathbf{r}_{n'}) \langle v_{n'} v_j \rangle, \quad (17)$$

where the line-of-sight velocity correlation $\langle v_{n'} v_j \rangle$ can be calculated in the same manner as Eq. (15).

Therefore, the only unknown in Eq. (13) is the Lagrange multiplier matrix λ . We can plug Eq. (13) into the constraint equation (9) to solve for λ_{pq} :

$$\lambda_{pq} = \sum_l \left[\sum_{ij} \langle S_j U_p \rangle G_{ij}^{-1} g_l(\hat{\mathbf{r}}_j) - \delta_{pl} \right] M_{lq}^{-1}, \quad (18)$$

where the matrix M is given by

$$M_{pq} = \frac{1}{2} \sum_{i,j} G_{ij}^{-1} (\mathbf{x}_p \cdot \mathbf{r}_i) (\mathbf{x}_q \cdot \mathbf{r}_j). \quad (19)$$

To summarise, by simulating an ideal survey at depth R and using Eqs. (14), (17), (18) and (19), one can calculate the weight function $w_{p,i}$ in Eq. (13) and hence obtain the bulk flow Moment at depth R according to Eq. (8).

Once we obtain the bulk flow moment from the minimum variance weighting scheme, we can calculate the covariance matrix and therefore perform a full statistical analysis. The covariance matrix of u_p becomes

$$\begin{aligned} C_{pq} &= \langle u_p u_q \rangle \\ &= \sum_{i,j} w_{p,i} w_{q,j} \langle S_i S_j \rangle \\ &= \sum_{i,j} w_{p,i} w_{q,j} G_{ij}, \end{aligned} \quad (20)$$

which can be broken down into an instrumental noise term

$$C_{pq}^n = \sum_i w_{p,i} w_{q,i} (\sigma_i^2 + \sigma_*^2), \quad (21)$$

and a cosmic variance term

$$C_{pq}^v = \frac{\Omega_m^{1.1} H_0^2}{2\pi^2} \int dk P(k) W_{pq}^2(k), \quad (22)$$

where the angle-averaged window function is

$$W_{pq}^2(k) = \sum_{i,j} w_{p,i} w_{q,j} F_{ij}(k). \quad (23)$$

This window function describes the scale in k -space that the catalogue actually probes. As an example, we plot this window function for the ENEAR catalogue at depth $50 h^{-1} \text{Mpc}$ in Fig. 2a. As expected, it matches the window function of ENEAR as shown in figure 3 in Watkins et al. (2009) perfectly well. The shape of the curves reveal that the window function decays rapidly for k beyond $0.05 h \text{Mpc}^{-1}$, therefore the non-linear regime of the matter power spectrum does not contribute to the bulk flow moment – bulk flow moments reflect perturbations on large scales, $k \lesssim 0.05 h \text{Mpc}^{-1}$.

3.3 Likelihood of Individual catalogues

Given the reconstructed bulk flow moment at some depth R and its covariance matrix C_{ab} (20), the likelihood of cosmological parameters θ is

$$\mathcal{L}(\theta) = \frac{1}{(2\pi)^{\frac{3}{2}} \det(C(\theta))^{\frac{1}{2}}} \exp\left(-\frac{1}{2} \sum_{p,q=1}^3 u_p C(\theta)_{pq}^{-1} u_q\right). \quad (24)$$

Since the major effect of the constraints is on the amplitude and shape of the matter power spectrum, in the following analysis we will only vary σ_8 and Ω_m , while fixing the other parameters at the *WMAP* values. We compute the bi-variate likelihood and marginalise one parameter to obtain the 1-D posteriori distribution of the other parameter.

In order to demonstrate the accurate reproduction of the results in Watkins et al. (2009), we use the same set of *WMAP* 5-year best-fit parameters (Komatsu et al. 2009): $\Omega_b = 0.0441$; $h = 0.719$; $n_s = 0.963$; $\tau = 0.087$; $A_s = 2.41 \times 10^{-9}$; plus small-scale velocity dispersion $\sigma_* = 150 \text{ km s}^{-1}$. We also use the approximation $\Gamma = \Omega_m h$ to calculate the matter power spectrum (see Appendix A for comparison with the numerical result), as is used in Watkins et al. (2009). In Fig. 2 we show that we can accurately reproduce the window function $W_{ab}^2(k)$ (see Eq. (23)) and marginalised distribution of σ_8 , as shown by the black line in Fig. 2b. These curves are very close to those shown as figures 3 and 7 of Watkins et al. (2009).

In addition, since we will not use the SBF, SC, SMAC, EFAR and Willick catalogues here, we need to test whether this ‘removal’ of data can substantially change the result. To do this, we use the rest of the data in the COMPOSITE catalogue, i.e. the combination of the SN, ENEAR and SFI++ catalogues (4256 samples in total), and keep all other conventions the same as in Watkins et al. (2009) to calculate the likelihood of σ_8 , and we obtain the red line in Fig. 2b. Comparing with the black line, one can see that the removal of these sparse and distant samples can move the peak of the likelihood towards lower values, but a very high value

of σ_8 is still preferred compared with the *WMAP* constraint (dashed line). Therefore, the excessive power in the bulk flow on $50 h^{-1} \text{Mpc}$ scales is not completely driven by the inclusion of five sparse and fairly noisy samples – we need to investigate further to understand the reasons.

We make the following adjustments to the model parameters in order to precisely compare the velocity field prediction with the observational data:

- we use *WMAP* 7-year best-fit cosmological parameters (Komatsu et al. 2011) to compute our prediction, i.e. $\Omega_b = 0.0455$, $h = 0.704$, $n_s = 0.967$, $\tau = 0.088$ and $A_s = 2.43 \times 10^{-9}$;
- we use the value $\sigma_* = 400 \text{ km s}^{-1}$ for the intrinsic velocity dispersion,² in order to compute the covariance matrix (Eq. (21)), since Ma et al. (2011) showed that this value is preferred for most catalogues;
- in the formula for $P(k)$, we use the numerical result from CAMB (Lewis, Challinor, & Lasenby 2000) instead of $\Gamma = \Omega_m h$ to compute the power spectrum, with the difference between the numerical result and the parameterisation $\Gamma = \Omega_m h$ being shown in Appendix A.

3.4 Combining catalogues: Bayesian hyper-parameter method

In Watkins et al. (2009), the combined catalogue, referred to as ‘COMPOSITE’ is used to reconstruct the bulk flow and constrain the cosmological parameters σ_8 and Ω_m . They found an excess power in the bulk flow on a scale of $50 h^{-1} \text{Mpc}$, which suggests a high value of σ_8 compared with the constraints from *WMAP* 5-year results (Komatsu et al. 2009) – see Fig. 2b.

Directly combining a variety of catalogues with different calibration methods and systematics may not be a precise way of exploring the combined constraints. Another way of carrying out the combination is to first compute the likelihood of individual data sets, and then directly combine them by multiplication, i.e.

$$\mathcal{L}_{\text{joint}}(\theta) = \prod_k^N \mathcal{L}_k(\theta), \quad (25)$$

where N is the number of data sets. Such a procedure assumes that the quoted observational random errors can be trusted, and that the two (or more) χ^2 statistics have equal weights, so that

$$\chi_{\text{joint}}^2 = \sum_k \chi_k^2. \quad (26)$$

However, when combining different data sets, one often wants to assign different weights to them. Lahav et al. (2000) describe an approach (see also Press 1997, for an earlier application of the same idea in astrophysics) using

$$\chi_{\text{joint}}^2 = \sum_k \alpha_k \chi_k^2, \quad (27)$$

where the α_k s are ‘hyper-parameters’, which are to be eval-

² Turnbull et al. (2012) used a thermal noise 250 km s^{-1} .

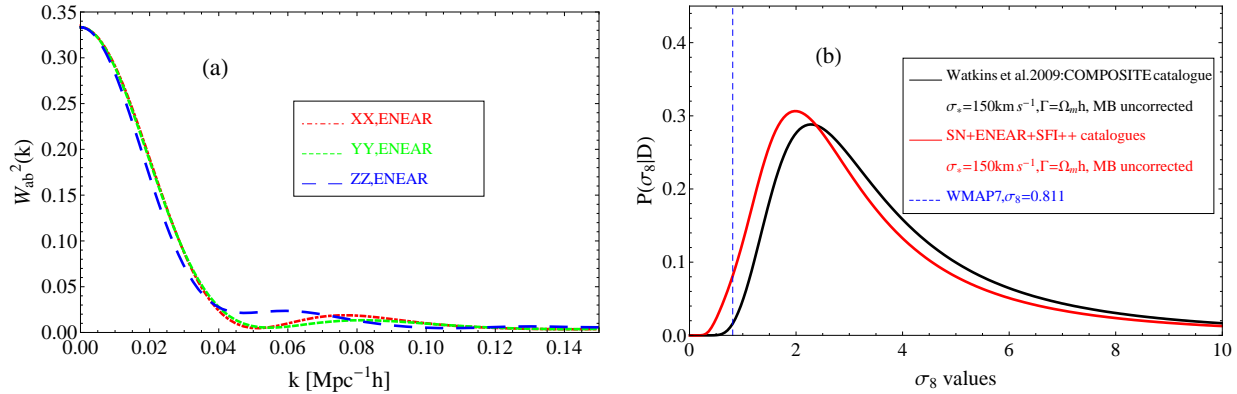


Figure 2. (a) Diagonal term of the window function $W_{ab}^2(k)$ (Eq. (23)) for the ENEAR catalogue at depth $50 h^{-1} \text{Mpc}$ (see Section 2.1 for a description of the catalogues). (b) Marginalised distribution of σ_8 for the COMPOSITE catalogue. The black line is obtained by adopting the conventions used in Watkins et al. (2009): no Malmquist bias correction; COMPOSITE catalogue (direct combination of SBF, SN, ENEAR, SFI++, EFAR, SC, SMAC and Willick); small scale velocity dispersion $\sigma_* = 150 \text{ km s}^{-1}$; and matter power spectrum parameter $\Gamma = \Omega_m h$. Note that this black line is produced by our own code and it matches figure 7 of Watkins et al. 2009 very well. The red line corresponds to the case where we use all these same conventions, but remove the SBF, EFAR, SC, SMAC and Willick catalogues.

uated in a Bayesian way. Here χ^2 for each data set is

$$\chi^2 = \sum_i \frac{[x_i^{\text{obs}} - x_i^{\text{the}}(\theta)]^2}{\sigma_i^2}, \quad (28)$$

where the summation is over N measurements and σ_i is the error for each data point. By multiplying χ^2 by α , each error σ_i effectively becomes $\alpha^{-\frac{1}{2}} \sigma_i$ and therefore if an experiment underestimates (or overestimates) the systematic errors, the hyper-parameter can scale the error by using relative weights. Indeed, the hyper-parameters are useful in assessing the relative weight for each different experiment. This procedure gives an objective diagnostic for revealing experiments with problematic error estimates and which therefore deserve further investigation of their systematic or random errors.

It is worth clarifying that, in principle, the systematic effects could have two different components, either an overall multiplicative factor for the velocities, or else an extra contribution to the measurement noise. Although the former kind of systematic effect would be appropriate for some other kinds of data (particularly where the dominant uncertainty is a linear calibration factor), the effect on the peculiar velocity field is more complicated than this. We therefore focus our attention on modelling the systematics as an additional source of noise, effectively giving a different weighting of the signal-to-noise of each data set. For a discussion of related issues in other branches of astrophysics see for example Gull (1989) and Stomp et al. (2009).

In the same spirit of assigning weights to each data set, Hobson et al. (2002) calculated the joint distribution of cosmological parameters for multiple data sets, in which the weight assigned to each is determined directly by its own statistical properties. The weights are considered in a Bayesian context as a set of hyper-parameters, which are then marginalised over in order to recover the posterior distribution as a function only of the cosmological parameters of interest. In the case of a Gaussian likelihood function, this marginalisation can be calculated analytically, and it is shown that the joint probability distribution, $P(D|\theta)$, when

applying the hyper-parameter approach is

$$\mathcal{L}_{\text{joint}}(\theta) = \prod_{k=1}^N \frac{2\Gamma\left(\frac{n_k}{2} + 1\right)}{\pi^{n_k/2} |V_k|^{1/2}} (\chi_k^2 + 2)^{-\left(\frac{n_k}{2} + 1\right)}, \quad (29)$$

where n_k , V_k and χ_k^2 are the number of data, covariance matrix and χ^2 for the k th data set. In our approach, flat priors on σ_8 and Ω_m are assumed. We will use Eq. (29) to explore the use of different catalogues to constrain cosmological parameters.

Once the distribution of Eq. (29) is calculated, the hyper-parameter is already marginalised over, which means that it automatically incorporates the relative weights between each data set and combines them in an objective way. Therefore, rather than using the COMPOSITE catalogue to constrain cosmology, we will first investigate the individual likelihoods for each data set, and use the joint distribution in Eq. (29) to combine these data sets.

4 RESULTS

In this section, we will perform two different analyses separately. The first one, in Section 4.1 and 4.2, will focus on reconstructing v_{bulk} on $50 h^{-1} \text{Mpc}$ scales, and use it to constrain cosmological parameters. In the second analysis, we will extend the ‘minimal variance’ scheme to consider the cumulative bulk flow at different radii, and to explore the joint constraints on cosmology from all the bulk flows in different shells.

4.1 Bulk flow moments

We now present our results on reconstructing bulk flow moments using the minimum variance method on $50 h^{-1} \text{Mpc}$ scales (Eq. (8)). In Fig. 3a, the magnitude of the bulk flow is plotted for the four different catalogues. Theoretically, the magnitude of bulk flow v follows the Maxwellian distribu-

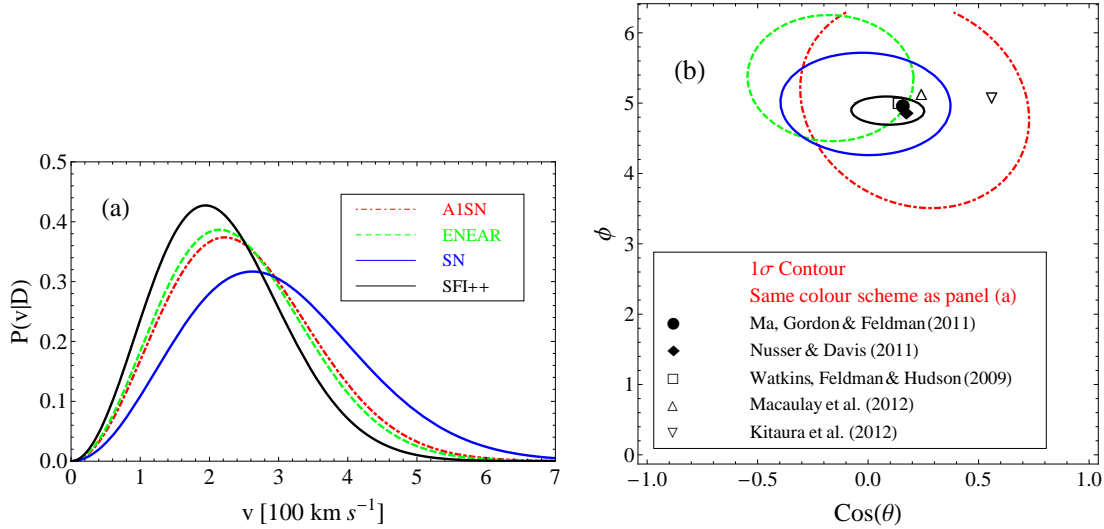


Figure 3. Bulk flow magnitude and direction (Eqs. (8) and (13)) for the ENEAR, SN, A1SN and SFI++ catalogues: (a) magnitude distribution; (b) 68% contours for the bulk flow direction, with $(\phi, \theta) = (l, \pi/2 - b)$. Bulk flow directions found by other probes and methods are also marked on the plot.

tion, i.e.

$$p(V)dV = \sqrt{\frac{54}{\pi}} \left(\frac{V}{\sigma_V}\right)^2 \exp\left[-\frac{3}{2}\left(\frac{V}{\sigma_V}\right)^2\right] \frac{dV}{\sigma_V}, \quad (30)$$

where σ_V is the velocity dispersion parameter (Coles & Lucchin 2002). We calculate it as $\sigma_V^2 = \sigma_x^2 + \sigma_y^2 + \sigma_z^2 = \sum_i C_{ii}$, where C is the covariance matrix (Eq. (20)). One can see that SFI++ provides the tightest constraint on the bulk flow magnitude; this is because it is the largest, densest and closest to full-sky survey available at the moment. In addition, ENEAR (669 samples) and A1SN (153 samples) provide roughly similar constraints on the bulk flow. This is due to the fact that although the A1SN (First Amendment Supernovae catalogue) has less data than ENEAR, its errors (calibrated by luminosity distance) are much smaller than for the Fundamental Plane distance estimates.

In Fig. 3a, one can also see that, although there are offsets between the peaks of the likelihood for each individual catalogue, they are all quite consistent with the theoretical prediction, which is the mean-squared velocity of a $50 h^{-1}\text{Mpc}$ spherical region of $v \simeq 310 \text{ km s}^{-1}$ (see Section 3.1). Therefore by correcting the inhomogeneous Malmquist bias and properly selecting the samples, the four catalogues show a coherent flow on $50 h^{-1}\text{Mpc}$ scales of about 310 km s^{-1} .

In addition, we plot the constraint on the direction of the bulk flow in Fig. 3b, and compare these directions with those found in other studies. From the figure, we can see that SFI++ provides the tightest constraint on the bulk flow direction, and the constraints on the direction of the bulk flows are consistent with each other across all catalogues. We also mark the preferred direction of the bulk flow from other published estimates. We can see that our constraints are consistent with the directions obtained from Ma et al. 2011, Nusser & Davis 2011, Watkins et al. 2009, and Macaulay et al. 2012, but Kitaura et al. (2012) prefer a slightly larger value for Galactic latitude.

	v [$\times 100 \text{ km s}^{-1}$]	l [degrees]	b [degrees]
ENEAR	2.2 ± 0.6	310 ± 30	-9.8 ± 14
A1SN	2.2 ± 0.7	290 ± 60	12.1 ± 20
SN	3.7 ± 1.1	290 ± 30	-0.7 ± 15
SFI++	3.4 ± 0.4	280 ± 8	5.1 ± 6

Table 2. ‘Minimal variance’ reconstructed magnitude and direction (Eq. (8)) for the four catalogues. The quoted error is the $\pm 1\sigma$ measurement error.

The quantitative results for the four catalogues are listed in Table 2.

4.2 Cosmological parameters

We now turn to cosmological parameter estimation. We first apply the likelihood function (Eq. (24)) to each individual catalogue to calculate $P(\sigma_8|D)$, assuming a flat prior, and then combine different catalogues by using the hyper-parameter joint likelihood function of Eq. (29). We show our results in Fig. 4.

In Fig. 4a, one can see that the posterior distribution for σ_8 is highly skewed and has a fairly long tail out to large amplitudes, which suggests that the peculiar velocity data available at the moment still cannot rule out flows with large amplitude. In addition, we can see that the SN catalogue peaks near the *WMAP* 7-year σ_8 value ($\sigma_8 = 0.811$), while the SFI++ catalogue prefers a slightly higher value and A1SN and ENEAR prefer smaller ones. However, within the errors they are all quite consistent with each other, and none of them are inconsistent with the *WMAP* value of σ_8 .

In Fig. 4b, we plot the constraints on the σ_8 – Ω_m plane by using the hyper-parameter likelihood function of Eq. (29). One can see that the *WMAP* best-fit value is located close to the 68% contour in the σ_8 – Ω_m plane, and therefore the hyper-parameter results are consistent with the expectation from ΛCDM . Comparing Fig. 4b with figure 6 in Watkins

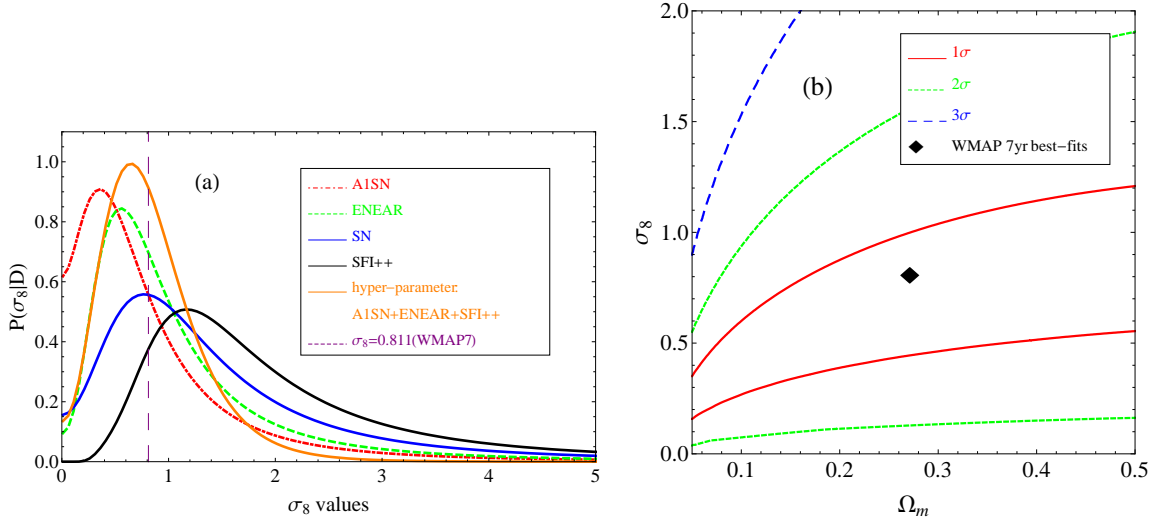


Figure 4. Cosmological parameter constraints: (a) the marginalised distribution of σ_8 , with the purple dashed vertical line showing the *WMAP* 7-year best fit σ_8 ; (b) 2-D contour plot in the σ_8 - Ω_m plane.

et al. (2009), one can see that our contour prefers a much lower value of σ_8 , and it is also closer to the *WMAP* value of Ω_m .

4.3 Multi-shells likelihood method

In the above approach, we use the reconstructed 3-D bulk flow velocity as the ‘observational data’ to constrain cosmology. We have shown that this likelihood (Eq. (24)) can provide a fairly strong constraint on σ_8 , but the constraint on Ω_m is rather weak and thus the 2-D contours of σ_8 - Ω_m do not close. This is because we use only one velocity vector (at $50 h^{-1}\text{Mpc}$) as a constraint and this information is not enough to provide a tight limit (see also figure 6 in Watkins et al. 2009).

Based on the ‘minimal variance’ scheme, here we propose another method to consider the bulk flow velocities for *all* of the shells within a certain radius. Since bulk flow velocities on different shells are highly correlated, one needs to calculate the full-covariance matrix of those bulk flow velocities. Note that we will apply this method to each individual data set to assess its validity for constraining cosmological parameters.

In the step of calculating $\langle S_j U_p \rangle$ (Eq. (17)), we need to simulate $N' = 10^4$ random velocities in the top-hat region R and therefore obtain the weighting function $w_{i,n}$ for a certain shell R . Let us assume we can sample multiple shells with this method, and therefore obtain the weighting function $w_{i,n}^R$ and bulk flow velocity u_i^R for each shell R . Now we can calculate the covariance matrix of u_i^R s as (R, R' are two shells)

$$\begin{aligned}
 C_{pq}^{RR'} &= \langle u_p^R u_q^{R'} \rangle \\
 &= \sum_{i,j} w_{p,i}^R w_{q,j}^{R'} \langle S_i S_j \rangle \\
 &= \sum_{i,j} w_{p,i}^R w_{q,j}^{R'} G_{ij},
 \end{aligned} \tag{31}$$

which can be broken down into an instrumental noise term

$$C_{pq}^{n,RR'} = \sum_i w_{p,i}^R w_{q,i}^{R'} (\sigma_i^2 + \sigma_*^2), \tag{32}$$

and a cosmic variance term

$$C_{pq}^{v,RR'} = \frac{\Omega_m^{1.1} H_0^2}{2\pi^2} \int dk P(k) \left(W_{pq}^{RR'} \right)^2(k), \tag{33}$$

where the angle-averaged window function is

$$\left(W_{pq}^{RR'} \right)^2(k) = \sum_{i,j} w_{p,i}^R w_{q,j}^{R'} F_{ij}(k). \tag{34}$$

Note that all of the shells are correlated. Suppose we have M shells, and now we arrange the bulk flow velocities of each shell into a $3 \times M$ velocity vector \tilde{u}_i , where i runs from 1 to $3M$. For instance, the y -direction of bulk flow in shell 3 is now at the position $3 \times (3-1) + 2 = 8$ in the \tilde{u}_i vector. We do the same thing for the covariance matrix, and therefore we turn the covariance matrix $C_{pq}^{RR'}$ into a $3M \times 3M$ covariance matrix $\Sigma = \Sigma^v + \Sigma^n$, where the Σ^v part contains the cosmological parameters and Σ^n includes measurement errors. Now the likelihood function for multiple shells becomes

$$\mathcal{L}(\theta) = \frac{1}{(2\pi)^{\frac{3}{2}} \det(\Sigma(\theta))^{\frac{1}{2}}} \exp \left(-\frac{1}{2} \sum_{i,j=1}^{3M} u_i \Sigma_{ij}^{-1} u_j \right). \tag{35}$$

We apply this likelihood function to the SFI++ and ENEAR catalogues, since they are the deeper catalogues with the broader sky-coverage. The SFI++ catalogue has a mean distance of $\sim 40 h^{-1}\text{Mpc}$ and extends out to $180 h^{-1}\text{Mpc}$, whereas the ENEAR catalogue has a mean distance $\sim 30 h^{-1}\text{Mpc}$ and goes out to $150 h^{-1}\text{Mpc}$. We first trim both data sets out to $100 h^{-1}\text{Mpc}$, which leaves 2830 (SFI++) and 690 (ENEAR) samples. Then we calculate the weighting functions $w_{i,n}$ and bulk flow velocities u_i for 8 different shells of distances 20 – $90 h^{-1}\text{Mpc}$, each with $10 h^{-1}\text{Mpc}$ separation. The reason we use the bulk flows only on shells with distances greater than $20 h^{-1}\text{Mpc}$ is that we would like to avoid non-linear structures on small scales.

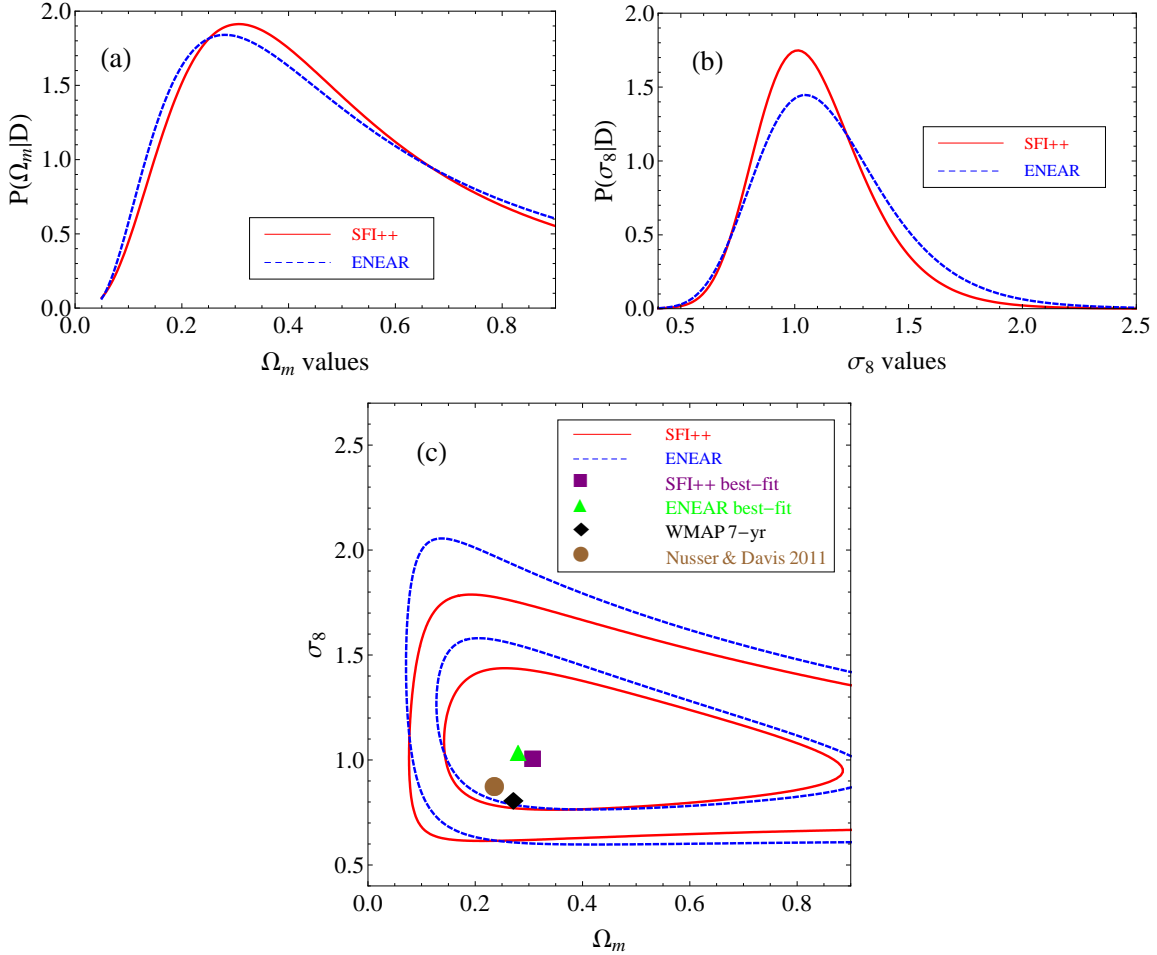


Figure 5. Marginalised distributions of σ_8 (panel (a)) and Ω_m (panel (b)) parameters from the SFI++ and ENEAR catalogues, by using the likelihood function (Eq. (35)) for 8 correlated shells with distances 20–90 h^{-1} Mpc. Panel (c) shows the 2-D contours of the joint distribution σ_8 – Ω_m . The *WMAP* 7-yr best-fit values and results from Nusser et al. (2011) are also plotted.

	Ω_m	σ_8	references
SFI++ multishells	$0.31^{+0.28}_{-0.14}$	$1.01^{+0.26}_{-0.20}$	This study
ENEAR multishells	$0.28^{+0.30}_{-0.14}$	$1.04^{+0.32}_{-0.24}$	This study
<i>WMAP</i> 7-year	0.271 ± 0.016	$0.811^{+0.030}_{-0.031}$	Komatsu et al. (2011)
SFI++ ASCE method	$0.235^{+0.16}_{-0.09}$	0.86 ± 0.11	Nusser & Davis (2011)

Table 3. Comparison on the constraints on cosmological parameters Ω_m and σ_8 from the multishell likelihood (Eq. (35)) and two other probes. Since Nusser et al. (2011a) do not explicitly quote the errors of the parameters, we roughly estimate the constraints from their figures 9 and 10.

In addition, more distant objects are not very well sampled and therefore are very sparse, so we restrict our bulk flows to within the shell of 90 h^{-1} Mpc. During the process of computation, we stick to the same conventions as listed in Section 3.3. Then we calculate the covariance matrix (Eq. (31)) and the likelihood function (Eq. (35)) for the 8 shells, and we obtain the marginalised distribution of Ω_m and σ_8 , as shown in Figs. 5a and 5b. The joint distribution of σ_8 – Ω_m is shown in Fig. 5c.

From Fig. 5a and Fig. 5c, one can see that the constraint on Ω_m becomes tighter than the previous single bulk flow constraint and its 1σ contour is now closed. Therefore,

by just using bulk flow data, one can obtain an independent constraint on the cosmological parameters. The best-fit value of *WMAP* 7-year results, as well as the constraints obtained from Nusser & Davis (2011) are all well within the $\pm 1\sigma$ confidence region of the parameter space. The reason that the likelihood function for multiple shells can give a reasonably good constraint on Ω_m , while the bulk flow at 50 h^{-1} Mpc does not, is that the dependence of $P(k)$ on Ω_m is a function of scale, and therefore by incorporating multiple shells, one can gain more information on perturbations at different depths.

We would also like to point out that since the current

peculiar velocity data are no deeper than $150 h^{-1}\text{Mpc}$, and the data beyond $100 h^{-1}\text{Mpc}$ are very noisy and sparse, the 8 shell bulk flows at distances of 20 to $90 h^{-1}\text{Mpc}$ are really the maximal information we can obtain with these catalogues. We have carefully checked that, for the data within $100 h^{-1}\text{Mpc}$, splitting into more shells of bulk flows does not improve the constraints, since these shells are highly correlated and we already have enough shells to effectively capture the scale dependence.

In addition, we should note that there is another statistical approach, the multiple moment method (Jaffe & Kaiser 1995; Feldman et al. 2010; Macaulay et al. 2011, 2012), which has been proposed to reconstruct the bulk flow, shear, and octupole moments of perturbations. This can be considered as an alternative method to our multishell likelihood approach. The multiple moment method used in Feldman et al. (2010) and Macaulay et al. (2011) considers perturbations only on $50 h^{-1}\text{Mpc}$ scales, but includes all moments, and they find that there is excessive power for the bulk flow, but not for the other moments. In contrast, our multishell likelihood function focuses just on the bulk flow, and it reconstructs this for shells of different distance, quantifying the full covariance matrix by calculating the correlations between shells. Our multishell likelihood shows that the bulk flow is not excessive compared with ΛCDM predictions, and that one can obtain reliable constraints on cosmological parameters by applying the method to various peculiar velocity catalogues.

We list the numerical results of our cosmological parameter constraints in Table 3.

5 DISCUSSION AND CONCLUSIONS

In this paper, we have been investigating bulk flow measurements using various catalogues. We find results which are different to those given by Watkins et al. (2009), who claimed evidence for a surprisingly large bulk flow on $50 h^{-1}\text{Mpc}$ scales, apparently discrepant with the ΛCDM prediction. In contrast, by carefully considering four selected catalogues, we find a coherent flow of about 300 km s^{-1} on a scale of $50 h^{-1}\text{Mpc}$, entirely consistent with the value expected given the *WMAP* 7-year cosmological parameters.

By employing the same weighting scheme and the same conventions, we are able to accurately reproduce the results in Watkins et al. (2009), as shown in Fig. 2. Since we focus on the SN, SFI++ and ENEAR catalogues, we removed the other sub-catalogues from the COMPOSITE catalogue, and found a slightly lower value of σ_8 (red line in Fig. 2b), but still higher than the *WMAP* constraint. This indicates that the high value of σ_8 inferred from the COMPOSITE catalogue is not completely driven by the five deep and sparse catalogues included (SMAC, SBF, SC, EFAR and Willick).

To summarise the various other issues which could be responsible for the discrepancy, in Table 4 we list several technical points which lead to quantitatively different results.

The first issue is the assumption of small-scale velocity dispersion, which goes into the calculation of the covariance matrix (Eq. (21)). Watkins et al. (2009) assumed a value of 150 km s^{-1} , which is too small compared to the constraint obtained by Ma et al. (2011, 2012a), which was closer to the

400 km s^{-1} we chose here. Besides this, Watkins et al. (2009) used an inaccurate approximation for the matter power spectrum. From Fig. A1, one can see that although this is a small effect, it has the same sign, yielding smaller flows. Thus, by fitting to the observed flows, this tends to further increase the normalisation parameter σ_8 .

The second major difference lies in the inhomogeneous Malmquist bias correction. In Watkins et al. (2009), only the SFI++ and SMAC catalogues were corrected for this effect. In our approach, we used the full-sky density field from the PSCz catalogue to extrapolate the density $n(r)$ at any spatial position, and calculate the probability of the true distance r given the measured distance d (Eq. (3)). The comparison between the measured distance/velocity and true distance/velocity in Fig. 1, shows that the bias tends to move galaxies to smaller distances.

Another difference is that we only keep the high quality samples SN, SFI++ and ENEAR from the Watkins et al. (2009) compilation, and we further include the recent compilation of supernovae data, i.e. the A1SN catalogue. To remove any possible bias from the distant and sparsely sampled region, we restricted our attention to $d \leq 80 h^{-1}\text{Mpc}$, and to avoid the results being driven by outliers, we also limited our samples to $|v| \leq 3000 \text{ km s}^{-1}$.

Furthermore, rather than using the COMPOSITE catalogue, we combined individual sample likelihoods using the Bayesian hyper-parameter technique. This should avoid the possibility that inconsistent data sets may bias the result if they are assigned equal weight. From the hyper-parameter likelihood, we find the best-fit value $\sigma_8 = 0.65^{+0.47}_{-0.35}$. This is somewhat low and hence inconsistent with a large bulk flow. However, the uncertainty is so large that this result is still consistent with standard ΛCDM expectations.

Finally, we proposed a multishell likelihood method, which calculates the bulk flows in all shells within a certain radius together with their covariance matrix. This multishell likelihood takes into account the scale-dependence of the matter power spectrum $P(k)$ on the Ω_m parameter, and therefore maximises the constraining power one can obtain from a data set. By applying this likelihood to the SFI++ and ENEAR catalogues, we showed that they can provide much stronger constraints on Ω_m and σ_8 than the single shell ($50 h^{-1}\text{Mpc}$) constraint. Our result also shows consistency with *WMAP* 7-year best-fits and results from Nusser & Davis (2011).

We conclude that the apparently large bulk flow on $50 h^{-1}\text{Mpc}$ scales found by Watkins et al. (2009) may not be a genuine flow. By correcting for Malmquist bias, carefully selecting samples and examining assumptions, one finds that the current peculiar velocity field catalogues are consistent with the ΛCDM model. On the other hand, any claimed discrepancy is not due to the ‘minimal variance’ scheme proposed by Watkins et al. (2009) and Feldman et al. (2010), since in our tests, we have shown that this scheme gives consistent results. In addition, our conclusions also agree with several other independent searches for bulk flows, such as the ASCE method with the SFI++ catalogue (Nusser & Davis 2011), the minimal variance method with the Type-Ia SN data (Turnbull et al. 2012), and the luminosity function method with the 2MRS samples (Branchini, Davis, & Nusser 2012). It should also be pointed out that the lack of evidence for a bulk flow on $50 h^{-1}\text{Mpc}$ removes some of the

	Watkins et al. (2009)	This study
Cosmological parameters	<i>WMAP</i> 5-year (Komatsu et al. 2009)	<i>WMAP</i> 7-year (Komatsu et al. 2011)
Small scale velocity dispersion σ_*	150 km s ⁻¹	400 km s ⁻¹
$P(k)$ calculation	Parameterisation with $\Gamma = \Omega_m h$	Numerical result from CAMB
Distance indicator	Malmquist bias uncorrected	Malmquist bias corrected
Catalogues	COMPOSITE: combination of SBF, SN, SFI++, ENEAR SC, SMAC, EFAR and Willick	SN, SFI++ and ENEAR catalogues
Data selection	None	Trim to $d \leq 80 h^{-1} \text{Mpc}$, $ v \leq 3000 \text{ km s}^{-1}$
Number of samples	COMPOSITE (4536)	SN (78), ENEAR (669), SFI++ (2404)
Combination method	Direct combination	Hyper-parameter likelihood & Multi-shell likelihood
Result for normalisation	$\sigma_8 = 1.7 \pm 0.28$ (excluded by <i>WMAP</i> at 99%)	$\sigma_8 = 0.65^{+0.47}_{-0.35}$ (hyper-parameter) $\sigma_8 = 1.01^{+0.26}_{-0.20}$ (SFI++) $\sigma_8 = 1.04^{+0.32}_{-0.24}$ (ENEAR) (consistent with <i>WMAP</i>)

Table 4. Comparison of the methodology, data selection, and results of our constraints with those in Watkins et al. (2009).

support for an excessive flow $\sim 1000 \text{ km s}^{-1}$ on even deeper scales $\sim 300 h^{-1} \text{Mpc}$ (Kashlinsky et al. 2008).

It seems clear that, despite extensive effort for decades, peculiar velocity catalogues remain systematics dominated. By applying different, but apparently reasonable, assumptions and statistical approaches, it is possible to find quite discrepant results using essentially the same data sets. This means that the realistic error bars are probably larger than given in many of the published studies. In addition, one should notice that there are many other methods developed to compute bulk flows that do not rely on distance indicators, such as luminosity fluctuations and fluctuations in the galaxy number density (Branchini, Davis, & Nusser 2012), as well as the use of the kinetic Sunyaev-Zeldovich effect (e.g. Osborne et al. 2011). Although they also suffer from systematic effects, these will be of a different nature and therefore such approaches can be regarded as complementary to the method discussed here. Large-scale bulk flows still offer promise for constraining cosmological models, but fully realising that promise will require further improvements in the construction of catalogues, and in the control of the systematic effects which continue to plague this field.

Acknowledgments: We would like to thank Michael Hudson and Stephen Turnbull for sharing with us the First Amendment Supernovae compilation, and Enzo Branchini and George Efstathiou for helpful discussions. This research was supported by the Natural Sciences and Engineering Research Council of Canada. YZM is supported by a CITA National Fellowship.

APPENDIX A: POWER SPECTRUM SEMI-ANALYTIC FORMULA ANALYSIS

To sample the σ_8 - Ω_m parameter space, we can apply a formula to generate the matter power spectrum $P(k)$. We use the following semi-analytic equation as presented in Eisenstein & Hu (1998):

$$P(k) = \sigma_8^2 k^{n_s} T(k)^2, \quad (\text{A1})$$

where

$$T(k) = \frac{L_0}{L_0 + C_0(k, \Gamma) (k/\Gamma)^2},$$

$$L_0 = \ln(2e + 1.8 (k/\Gamma)),$$

$$C_0(k, \Gamma) = 14.2 + \frac{731}{1 + 62.5 (k/\Gamma)}. \quad (\text{A2})$$

The quantity Γ here is called the power spectrum ‘shape parameter’. Watkins et al. (2009) and Feldman et al. (2010) used $\Gamma = \Omega_m h$ as an approximation on large scales. However, in Fig. A1, we can see that this approximation ($P_1(k)$) still has relatively large deviations from the numerical result from CAMB.

A more accurate parameterisation of the shape parameter is $\Gamma = \Omega_m h \exp(-\Omega_b(1 + \sqrt{2h}/\Omega_m))$, as advocated in Eisenstein & Hu (1998). This is much closer to the numerical $P(k)$, due to the additional exponential factor.

In order to demonstrate the successful reproduction of results in Watkins et al. (2009), we use the approximation $\Gamma = \Omega_m h$ in Section 3. However, since in our subsequent analysis, we need to carefully compare the numerical value of the reconstructed bulk flow moment with the expectation based on cosmological parameters, we switch to the numerical result of the $P(k)$ from CAMB (Lewis, Challinor, & Lasenby 2000) in our determination of the bulk flow moments in each individual catalogue and subsequent hyper-parameter analysis.

REFERENCES

- Abate A., Erdogdu P., 2009, MNRAS, 400, 1541
Bernardi M. et al., 2002, AJ, 123, 2990
Bouchet F.R., Lachièze-Rey M., eds., 1993, ‘Cosmic Velocity Fields’, Editions Frontieres, Gif-sur-Yvette
Branchini E., Davis M., Nusser A., 2012, MNRAS, 424, 472
Burstein D., 1990, Rep. Prog. Phys., 53, 421
Courteau S., Faber S. M., Dressler A., Willick J. A., 1993, ApJ, 412, 51
Coles P., Lucchin F., Cosmology– The Origin and Evolution of Cosmic Structure. John Wiley & Sons, LTD, 2002
Colless M. et al., 2001, MNRAS, 321, 277
Courteau S., Willick J., eds., ‘Cosmic Flows Workshop’,

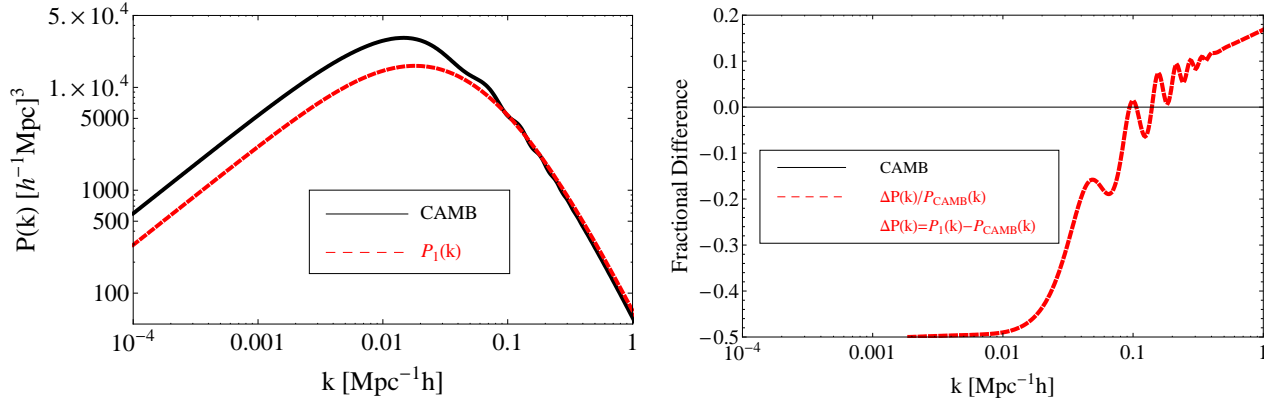


Figure A1. Comparison of the approximation $P_1(k)$ using shape parameter $\Gamma = \Omega_m h$ with the numerical result from CAMB (Lewis, Challinor, & Lasenby 2000). Here we adopt *WMAP* 5-year best-fit parameters (Komatsu et al. 2009). One can see that there are large deviations on scales of 10^{-4} to $0.1 h\text{Mpc}^{-1}$.

2000, ASP Conf. Ser., Vol. 201, Astronomical Society of the Pacific, San Francisco
da Costa L.N. et al., 2000, AJ, 120, 95
Dale D.A. et al., 1999, AJ, 118, 1489
Eisenstein D, Hu W., 1998, ApJ, 496, 605
Feldman H., Watkins R., Hudson M.J., 2010, MNRAS, 407, 2328
Folatelli G. et al., 2010, AJ, 139, 120
Giovannelli R. et al., 1998, AJ, 116, 2632.
Gull S.F., 1989, in ‘Maximum Entropy and Bayesian Methods’, ed. J. Skilling, Kluwer Academic Publishers, Dordrecht, p. 53
Hendry M.A., Simmons J.F.L., Newsam A.M., 1993, in ‘Cosmic Velocity Fields’, ed. M. Lachièze-Rey, F. Bouchet, Editions Frontieres, Gif-sur-Yvette, p. 23
Hicken M. et al., 2009, ApJ, 700, 1097
Hobson M.P., Bridle S.L., Lahav O., 2002, MNRAS, 335, 377
Hudson M.J., 1994, MNRAS, 266, 468
Hudson M.J., 1999, PASP, 111, 57
Hudson M.J., Smith R.J., Lucey J.R., Branchini E., 2004, MNRAS, 352, 61
Jaffe A.H., & Kaiser N., 1995, ApJ, 455, 26
Jha S., Riess A.G., Kirshner R.P., 2007, ApJ, 659, 122
Juszkiewicz R., Vittorio N., Wyse R.F.G, 1990, ApJ, 349, 408
Kashlinsky A., Atrio-Barandela F., Kocevski D., Ebeling, H., 2008, ApJ, 686, 49
Kitaura F.-S. et al., 2012, 1205.5560 [arXiv:astro-ph]
Komatsu E. et al., 2009, ApJS, 180, 330
Komatsu E. et al., 2011, ApJS, 192, 18
Lahav O. et al., 2000, MNRAS, 315, 45
Latham D.W., da Costa L.A.N., eds., ‘Large Scale Structures and Peculiar Motions in the Universe’, ASP Conf. Ser., Vol. 15, astronomical Society of the Pacific, San Francisco
Lewis A., Challinor A., Lasenby A., 2000, ApJ, 538, 473
Lynden-Bell D., Faber S.M., Burstein D., Davis R.L., Dressler A., Terlevich R.J., Wegner G., 1988, ApJ, 326, 19
Ma Y.Z., Gordon C., Feldman H., 2011, Phys. Rev., D83, 103002

Ma Y.Z., Ostriker J., Zhao G.B., 2012a, JCAP, 06, 026
Ma Y.Z., Branchini E., Scott D., 2012b, MNRAS, 425, 2880
Macauley E., Feldman, H., Ferreira, P.G., Hudson, M.J., Watkins, R., 2011, MNRAS, 414, 621
Macauley E. et al., 2012, MNRAS, 425, 1709
Malmquist K., 1920, Medd. Lund. Astron. Obs., 22, 1
Nusser A., Davis M., 2011, ApJ, 736, 93
Osborne S.J., Mak D.S.Y., Church S.E., Pierpaoli, E., 2011, ApJ, 737, 98
Peebles P.J.E., Principles of Physical Cosmology. Princeton University Press, 1993
Press W.H., 1997, in ‘Unsolved Problems in Astrophysics’, ed. Bahcall J.N., Ostriker J.P., Princeton University Press, p. 49
Sarkar D., Feldman H.A., Watkins R., 2007, MNRAS, 375, 691
Springob C.M. et al., 2007, ApJS, 172, 599
Stompor R., Leach S., Stivoli F., Baccigalupi C., 2009, MNRAS, 392, 216
Strauss M.A., Willick J.A., 1995, Phys. Rep., 261, 271
Tonry J.L. et al., 2001, ApJ, 546 681
Tonry J.L. et al., 2003, ApJ, 594, 1
Turnbull S.J., Hudson M.J., Feldman H.A., Hicken M., Kirshner R.P., Watkins R., 2012, MNRAS, 420, 447
Watkins R., Feldman H.A., Hudson M.J., 2009, MNRAS, 392, 743
Wenger G. et al., 2003, AJ, 126, 2268
Willick J.A., 1999, ApJ, 522, 647